Frontiers in Bioscience Landmark

Front. Biosci. (Landmark Ed) **2026**; 31(1): 47089
https://doi.org/10.31083/FBL47089

Original Research

Integrated Single-Cell and Bulk RNA Sequencing Identifies SERPING1 as a Biomarker of Immune Infiltration and Prognosis in Triple-Negative Breast Cancer

Yuhang Shang[1], Runze Guo[2], Jiangwei Liu[1], Weilun Cheng[1], Anbang Hu[1], Yansong Liu[1], Yunqiang Duan[1], Xuelian Wang[1], Zhengbo Fang[1], Yanling Li[1], Hanyu Zhang[1], Mingcui Li[1], Zhiyuan Rong[1], Yuanhao Ji[1], Yulin Chen[1], Delong Cui[1], Yunyi Ji[1], Baoliang Guo[1,*]

[1]Department of General Surgery, The Second Affiliated Hospital of Harbin Medical University, 150081 Harbin, Heilongjiang, China
[2]School of Basic Medicine, Harbin Medical University, 150081 Harbin, Heilongjiang, China
*Correspondence: baoliangguo2020@hrbmu.edu.cn (Baoliang Guo)
Academic Editor: Jordi Sastre-Serra
Submitted: 2 October 2025 Revised: 9 December 2025 Accepted: 17 December 2025 Published: 22 January 2026

Abstract

Background: Triple-negative breast cancer (TNBC) is an aggressive malignancy that lacks effective treatment. Immune infiltration plays an important role in anti-tumor responses. Serpin family G1 (*SERPING1*), a biomarker associated with immune infiltration, has been implicated in multiple cancers, but its role in TNBC remains unclear. **Methods**: RNA sequencing and clinical data for TNBC were obtained from the Gene Expression Omnibus, the Cancer Genome Atlas, and the Molecular Taxonomy of Breast Cancer International Consortium databases. First, the expression, prognostic value, and biological functions of *SERPING1* were analyzed. Then, the tumor microenvironment (TME) was comprehensively characterized, and the relationship between *SERPING1* expression and immunotherapy response was assessed. Immunohistochemical staining was performed to confirm SERPING1 expression and the abundance of CD4+ T cells and CD8+ T cells in clinical specimens. Finally, single-cell analysis was conducted to investigate the role of *SERPING1* in immune cell activation. **Results**: *SERPING1* was downregulated in TNBC and was an independent predictor of survival. Functionally, *SERPING1* activated the immune response in TNBC patients. Mechanistically, elevated *SERPING1* levels lead to increased immune cell infiltration, particularly of CD4+ and CD8+ T cells, in the TME. Moreover, *SERPING1* was primarily localized in cancer-associated fibroblasts (CAFs), with SERPING1+ apCAFs exhibiting increased communications with anti-tumor immune cells at the single-cell level. **Conclusions**: *SERPING1* contributes to enhanced immune cell infiltration, desirable immunotherapy response, and improved prognosis. It thus can be utilized as a promising biomarker for immune infiltration and prognosis. These findings provide novel insights into TME-related immune regulation and may inform strategies to enhance immunotherapy efficacy in TNBC.

Keywords: triple negative breast neoplasms; tumor microenvironment; immunomodulation; prognosis; biomarker; immunotherapy

1. Introduction

Breast cancer (BC) is the most common malignancy among women globally, with triple-negative breast cancer (TNBC) accounting for approximately 15–20% of cases. TNBC is associated with a particularly poor prognosis, characterized by its high histological grade and increased rates of metastasis [1]. Due to the absence of estrogen receptor (ER), progesterone receptor (PR), and human epidermal growth factor receptor 2 (HER2) expression, TNBC is unresponsive to endocrine and HER2-targeted therapies [2]. As a result, surgery and chemotherapy remained the standard treatments for TNBC patients over the past decades [3].

In recent years, immune checkpoint inhibitors (ICI) have achieved some success across multiple tumor types [4,5]. As the most immunogenic subtype of BC, TNBC has demonstrated clinical benefit from immunotherapy. The programmed cell death ligand 1 (PD-L1, also known as CD274) blocking antibodies, atezolizumab and pembrolizumab, combined with chemotherapy, have been approved as first-line treatment for PD-L1-positive metastatic TNBC [6–8]. However, due to limited expression of PD-L1 and substantial heterogeneity of TNBC tumor microenvironment (TME), not all patients benefit from ICI treatment, and approximately 60%–85% of them develop primary resistance to ICI monotherapy [8,9]. Therefore, there is an urgent need to explore novel therapeutic targets and enhance the efficacy of immunotherapy in TNBC.

Currently, research on solid tumors has shifted from focusing solely on tumor cells to encompassing the TME [10]. Tumor-infiltrating lymphocytes (TILs) play a critical role in treatment response and prognosis, serving as key determinants of immunotherapy efficacy [11]. However, TME comprises not only lymphocytes but also stromal cells, immunosuppressive cells, extracellular matrix (ECM), and other components [12]. Increasing evidence indicates that cancer cells do not act alone but interact closely with different cell populations and ECM [13]. The ECM,

as a key structural and supportive component of the TME, constitutes more than 90% of breast tumors. Among its constituents, cancer-associated fibroblasts (CAFs) are the most abundant cell type, characterized by marked heterogeneity and plasticity [14,15]. CAFs profoundly influence tumor growth, invasion, and immune responses through ECM remodeling, metabolic regulation, and signaling interactions with both tumor and immune cells [16]. With the deepening of research on TME, novel targets correlated with immune infiltration have been identified [17]. These discoveries offer new opportunities to improve cancer treatment, particularly by enhancing immunotherapy and strengthening host anti-tumor immune responses.

SERPING1, located on chromosome 11, encodes the C1-inhibitor, a highly glycosylated plasma protein that regulates the complement cascade, as well as fibrinolytic, clotting, and kinin pathways. It plays a crucial role in controlling vascular permeability and innate immunity [18]. Recently, *SERPING1* has gained attention for its involvement in tumor biology and the TME [19]. Evidence indicated that *SERPING1* was downregulated in liver cancer cells, with low expression linked to an immunosuppressive TME and poor prognosis [20]. Similarly, the anti-cancer role of *SERPING1* was also demonstrated in gastric and prostate cancers [21,22]. However, limited knowledge exists regarding the distinct roles of *SERPING1* in TNBC, particularly in relation to TME and immune status, highlighting the need for further investigation.

Herein, we conducted a comprehensive investigation focusing on the function of *SERPING1* in TNBC. We noticed that *SERPING1* expression was significantly downregulated in TNBC compared with normal tissue, with low *SERPING1* levels associated with poor prognosis and diminished responses to immunotherapy. Mechanistically, *SERPING1* regulated the infiltration of various immune cells, especially T lymphocytes. Overall, our findings provided a thorough understanding of the complex roles of *SERPING1* in TNBC and highlighted its potential as a predictive biomarker in clinical practice.

2. Material and Methods

2.1 Datasets

Gene expression profiles and clinicopathological information were downloaded from the Cancer Genome Atlas (TCGA) data portal. Single-cell RNA sequencing (scRNA-seq) data (GSE176078) were obtained from the Gene Expression Omnibus (GEO) database. External validation was performed using data from Molecular Taxonomy of Breast Cancer International Consortium (METABRIC), Kaplan-Meier plotter (KM plotter: https://kmplot.com/analysis/) and GEO datasets (GSE45827, GSE103091). Proteomic expression of SERPING1 was analyzed via UALCAN [23]. The immunotherapy response data were derived from GSE91061 dataset and IMvigor210 cohort.

2.2 Identification of Differentially Expressed Genes

RNA-seq data from 118 TNBC and 99 normal samples from TCGA were selected for analysis. Using the "DESeq2" package (version 1.40.2), 5239 differentially expressed genes (DEGs) were identified with $|\log2(\text{fold change})| > 1$ and $p < 0.05$, including 2906 upregulated and 2333 downregulated genes. Multiple testing was corrected using the Benjamini-Hochberg false discovery rate (FDR) method. Further comparison between low and high *SERPING1* expression groups revealed 200 upregulated and 595 downregulated genes.

2.3 Immune Infiltration Analysis

ESTIMATE algorithm was used to calculate the tumor purity and immune scores of TNBC samples in TCGA cohort [24]. xCell, quanTIseq, MCPcounter, CIBERSORT Absolute, and EPIC algorithms were implemented using the "IOBR" R package (version 0.99.8). The relationship between *SERPING1* expression and the tumor infiltration status of 29 immune gene sets was assessed using the ssGSEA algorithm [25]. Moreover, the TIMER algorithm(http://cistrome.org/TIMER/) was utilized to investigate the correlations between *SERPING1* expression and CD4+ and CD8+ T cell infiltration in basal BC [26].

2.4 Immune Checkpoints and Immunotherapy Response Estimation

Major histocompatibility complex (MHC) molecules and immune checkpoints were compared between the high and low *SERPING1* expression groups [27]. Immunophenoscore (IPS) scores from The Cancer Immunome Atlas (TCIA) (https://tcia.at/home) and tumor immune exclusion score from TIDE algorithm (http://tide.dfci.harvard.edu/) were assessed to evaluate tumor immunogenicity [28,29].

2.5 Screening for the Hub Genes Associated With Immune Infiltration

Weighted Gene Co-expression Network Analysis (WGCNA) was conducted using the "WGCNA" R package on TNBC samples from the TCGA database [30]. Hierarchical clustering was performed based on gene expression, identifying genes with high similarity within modules using the dynamic cut tree method. The Module Eigengene (ME) value for each module and its correlation coefficients with ESTIMATE scores were calculated. A soft thresholding power of 3 was selected. The minimum module size was set at 30. Then, least absolute shrinkage and selection operator (LASSO) COX regression analysis was used to determine the final hub genes associated with immune infiltration.

2.6 Functional Enrichment Analysis

To annotate potential biological processes associated with *SERPING1*, we performed enrichment analysis using

Gene Ontology (GO) (http://geneontology.org/) and Kyoto Encyclopedia of Genes and Genomes (KEGG) (https://www.kegg.jp/), with the "ClusterProfiler" R package (version 4.8.2). Multiple testing was corrected using the Benjamini-Hochberg FDR method. GO analysis was conducted based on 3 categories, including biological process (BP), molecular function (MF), and cellular component (CC). Additionally, Gene Set Enrichment Analysis (GSEA) was performed as a secondary step, where it evaluates sets of biologically relevant genes, such as those in specific pathways, and categorizes gene groups based on their enrichment scores.

2.7 Patients and Tissue Specimens

A total of 18 TNBC samples and 28 normal breast tissue samples were collected from the Second Affiliated Hospital of Harbin Medical University (HMU). Informed consent was obtained from all participants, and the study was approved by the Ethics Committee of HMU. All samples were diagnosed by a minimum of 3 pathologists, and the tissue microarray was conducted following standard procedures. All research was performed following the Declaration of Helsinki.

2.8 Immunohistochemical Staining

The tissue microarrays were immunostained as described previously [31]. The anti-SERPING1 (1:50, 12259-1-AP, Rabbit, Proteintech, Wuhan, China), anti-CD8 (1:200; HPA037756; Merck KGaA, Darmstadt, Germany) and anti-CD4 (1:50; ab231460; Abcam, Shanghai, China) were used as primary antibodies. Staining intensity was scored from 0 to 3, with 0 indicating no staining, 1 indicating light brown, 2 indicating brown, and 3 indicating tan. The extent of staining was rated from 0 to 4 based on the percentage of positive cells: 0–25%, 25–50%, 50–75%, and 75–100%. The immunohistochemistry (IHC) score was calculated as the product of staining intensity and extent scores, yielding a range from 0 to 12. Scores 0–4 were assigned as negative, and scores 5–12 were assigned as positive [32]. The percentages of CD4+ and CD8+ T cells in each TNBC sample were determined by analyzing at least five 40$\times$ field-of-view regions. The sections were independently reviewed by two pathologists.

2.9 ScRNA-seq Analysis

GSE176078 was conducted using the R package "Seurat" according to standard procedures. We used the harmony dimensionality reduction algorithm to de-batch the 9 TNBC samples. We visualized the dimensionality reduction via the "UMAP" function, and all cells were annotated based on reference datasets from the CellMarker 2.0 (http://bio-bigdata.hrbmu.edu.cn/CellMarker/). Intercellular communications were computed by the R package "CellChat", which leverages a receptor-ligand interaction database.

2.10 Statistical Analysis

Statistical analyses were conducted using R software (version 4.3.1; R Foundation for Statistical Computing, Vienna, Austria). Categorical variables were assessed using the χ^2 test. A paired t test was used for paired analysis of TCGA samples. Quantitative data were tested for normal distribution and variance homogeneity using the Kolmogorov-Smirnov method. Differences between groups were analyzed using the Wilcox test. Survival data were analyzed using Kaplan-Meier (KM) curves, the log-rank test, and both univariate and multivariate Cox regression analyses. Pearson's test was carried out for correlation analysis. A p-value of less than 0.05 was considered statistically significant. All plots were generated using R software.

3. Results

3.1 SERPING1 was a Hub Gene Related to Immune Infiltration in TME

A total of 5239 DEGs were identified between TNBC and normal tissues in TCGA database, including 2906 upregulated and 2333 downregulated genes (Fig. 1A). ESTIMATE algorithm was applied to assess the level of infiltration of immune and stromal cells in each TNBC sample (**Supplementary Table 1**). DEGs and results of ESTIMATE were then incorporated into the WGCNA in search of immune infiltration-related biomarkers. 8 co-expression modules were recognized with a power of 3 as the optimal soft threshold (Fig. 1B,C). Based on Pearson's correlation coefficient, a heat map illustrating module-trait relationships was drawn to assess the relationships between modules. The turquoise module exhibited the highest correlation with immune infiltration scores and was designated as an "immune infiltration-related DEGs (IRDEGs) module" (Fig. 1D,E). Univariate Cox regression analysis of the 1239 IRDEGs in turquoise module identified 46 genes significantly associated with overall survival (OS) ($p < 0.05$; **Supplementary Table 2**). Subsequently, these significant genes were subjected to LASSO COX regression analysis and eleven crucial genes, namely, *NUAK2*, *ANKDD1B*, *ACSS2*, *RASGRP1*, *SDS*, *SERPING1*, *ZBED6CL*, *HLA-DQB2*, *PRDM12*, *ZNF296* and *PEG10* were generated (Fig. 1F,G and **Supplementary Table 3**). *SERPING1*, which has not been previously reported in TNBC, was selected as a candidate target for further investigation.

3.2 Downregulation of SERPING1 was Associated With Advanced Tumor Stage and Poor Prognosis in TNBC

Unpaired and paired analyses of TCGA cohort revealed that *SERPING1* was significantly downregulated in cancer tissues compared to normal tissues (Fig. 2A). Consistent results were observed in the GSE45827 dataset (Fig. 2B). To validate the expression of SERPING1, we constructed a tissue array consisting of 18 TNBC samples and 28 normal samples from patients in our department and

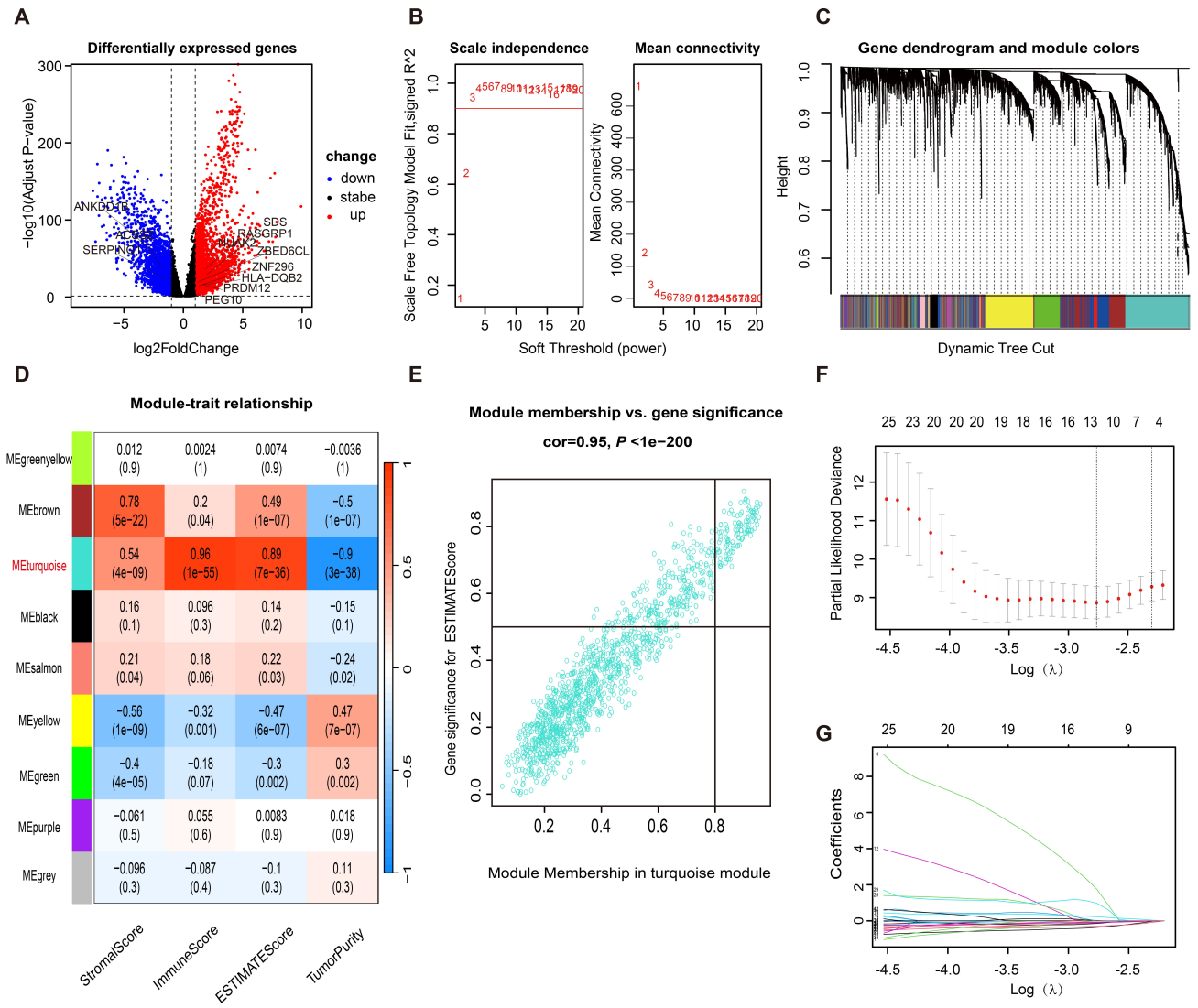

Fig. 1. Identification of hub genes associated with immune infiltration for TNBC. (A) Volcano plot of DEGs of normal and TNBC samples in TCGA cohort. Weighted gene co-expression network analysis: (B) Analysis of network topology for soft powers; (C) Cluster dendrogram developed by the weighted correlation coefficients, genes with similar expression patterns were clustered into co-expression modules, and each color represents a module; (D) The heatmap of module-trait relationships; (E) Correlation Curve of turquoise module. (F,G) LASSO COX regression of eleven immune infiltration-related DEGs. TNBC, triple-negative breast cancer; DEGs, differentially expressed genes; TCGA, the Cancer Genome Atlas; LASSO, least absolute shrinkage and selection operator.

performed IHC staining. The IHC scores confirmed significantly lower expression of SERPING1 in TNBC compared to normal tissues (Fig. 2C). KM survival analysis from TCGA cohort demonstrated that low *SERPING1* group showed inferior OS than high *SERPING1* group (Fig. 2D). Both univariate and multivariate Cox regression analyses confirmed that *SERPING1* served as an independent prognostic factor for OS in TNBC patients (Table 1). These findings were corroborated by analyses of the METABRIC and GSE103091 cohorts (Fig. 2E and **Supplementary Fig. 1**). Additionally, among different BC subtypes, the lowest expression of SERPING1 mRNA and protein was observed in TNBC (Fig. 2F and **Supplementary Fig. 2**). Further validation using KM plotter database indicated that higher *SERPING1* expression was associated with improved survival only in basal BC, which includes the majority of TNBC (Fig. 2G–J). Moreover, low *SERPING* expression was significantly correlated with large tumor size and advanced tumor stage (Fig. 2K–N). These findings highlighted that *SERPING1* may serve as a positive prognostic biomarker in TNBC.

3.3 Functional Enrichment Analysis of SERPING1 in TNBC

Limited evidence exists regarding the biological characteristics of *SERPING1* in malignancies, particularly in TNBC. Therefore, GO and KEGG enrichment analyses using the DEGs between low and high *SERPING1* groups

Table 1. Univariate and Multivariate COX regression analysis of OS in TCGA database.

Variables	Overall survival			
	Univariate		Multivariate	
	HR (95% CI)	*p*-value	HR (95% CI)	*p*-value
Age at diagnosis (%)				
<65 years	ref			
≥65 years	1.75 (0.56, 5.43)	0.332		
T				
T1	ref		ref	
T2	2.47 (0.53, 11.38)	0.247	1.55 (0.32, 7.56)	0.589
T3–4	5.88 (1.07, 32.28)	0.041	1.51 (0.24, 9.43)	0.661
N				
N0	ref		ref	
N+	4.17 (1.47, 11.86)	0.007	4.52 (1.48, 13.77)	0.008
Stage*				
Stage I–II	ref			
Stage III–IV	5.30 (2.01, 14.01)	0.001		
Histology type				
IDC	ref			
ILC	5.87 (0.74, 46.30)	0.093		
Other	1.29 (0.33, 5.00)	0.710		
SERPING1 expression	0.50 (0.30, 0.83)	0.008	0.47 (0.27, 0.84)	0.010

OS, Overall survival; HR, Hazard ratio; CI, Confidence interval; ref, Reference; IDC, Invasive ductal carcinoma; ILC, Invasive lobular carcinoma. *p*-value was considered statistically significant. * Stage was not enrolled in multivariate analysis because it is related to T and N.

were conducted to annotate their functions and investigate the role of *SERPING1*. The results highlighted the crucial role of *SERPING1* in immune regulation. GO enrichment analysis indicated that *SERPING1* was associated with essential BP such as leukocyte-mediated immunity, lymphocyte-mediated immunity and activation of immune response. Moreover, *SERPING1* was linked to specific CC, such as the immunological synapse and MHC protein complex, both crucial for T cell activation. MF analysis revealed enrichment in receptor ligand activity, cytokine activity, immune receptor activity, and cytokine binding, underscoring its functional contribution to immune regulation (Fig. 3A). KEGG pathway analysis also revealed the involvement of *SERPING1* in immune signaling, such as cytokine-cytokine receptor interaction pathway and T cell receptor signaling pathway (Fig. 3B). Consistently, GSEA demonstrated significant enrichment of immune response-related pathways in the high *SERPING1* group (Fig. 3C).

3.4 High Expression of SERPING1 was Associated With Inflamed TME

To better understand the impact of *SERPING1* on immune cells within TME, immune cell infiltration analysis was conducted using the "Xcell" algorithm. High *SERPING1* group presented lower tumor purity and higher percentage of anti-tumor immune cells, including CD8+ T cells, CD4+ memory T cells, B cells, macrophages M1 and activated dendritic cells (DC) (Fig. 4A). These findings were validated using other reliable algorithms (Fig. 4B and **Supplementary Fig. 3A–C**). Moreover, ssGSEA analysis of immune function scores revealed an activated immune status in the high *SERPING1* group (Fig. 4C). Given that the enrichment analysis predominantly highlighted T cell-related pathways (regulation of T cell activation, T cell receptor signaling pathway, and Th1 and Th2 cell differentiation) and that *SERPING1* demonstrates a positive correlation with CD4+ T cells and CD8+ T cells, we hypothesize that *SERPING1* may inhibit tumorigenesis by promoting the infiltration of protective immune cells, particularly T cells (Fig. 4D). Tissue microarrays were prepared from the same batch in our department, ensuring that samples sharing the same ID number had similar background tissue characteristics. Two well-prepared tissue microarrays were subjected to IHC staining for CD4 and CD8. As shown in Fig. 4E, the high SERPING1 expression context exhibited a greater abundance of infiltrating CD4+ T cells and CD8+ T cells. These observations indicated that *SERPING1* overexpression was associated with an inflamed TME in TNBC.

3.5 SERPING1 Expression Could Predict the Clinical Immunotherapy Efficacy of TNBC

We next investigated whether *SERPING1* could predict patient response to ICI therapy. ICI response biomarkers, including MHC molecules and immune checkpoints, were all elevated in the high *SERPING1* group (Fig. 5A). In addition, patients with high *SERPING1* expression ex-

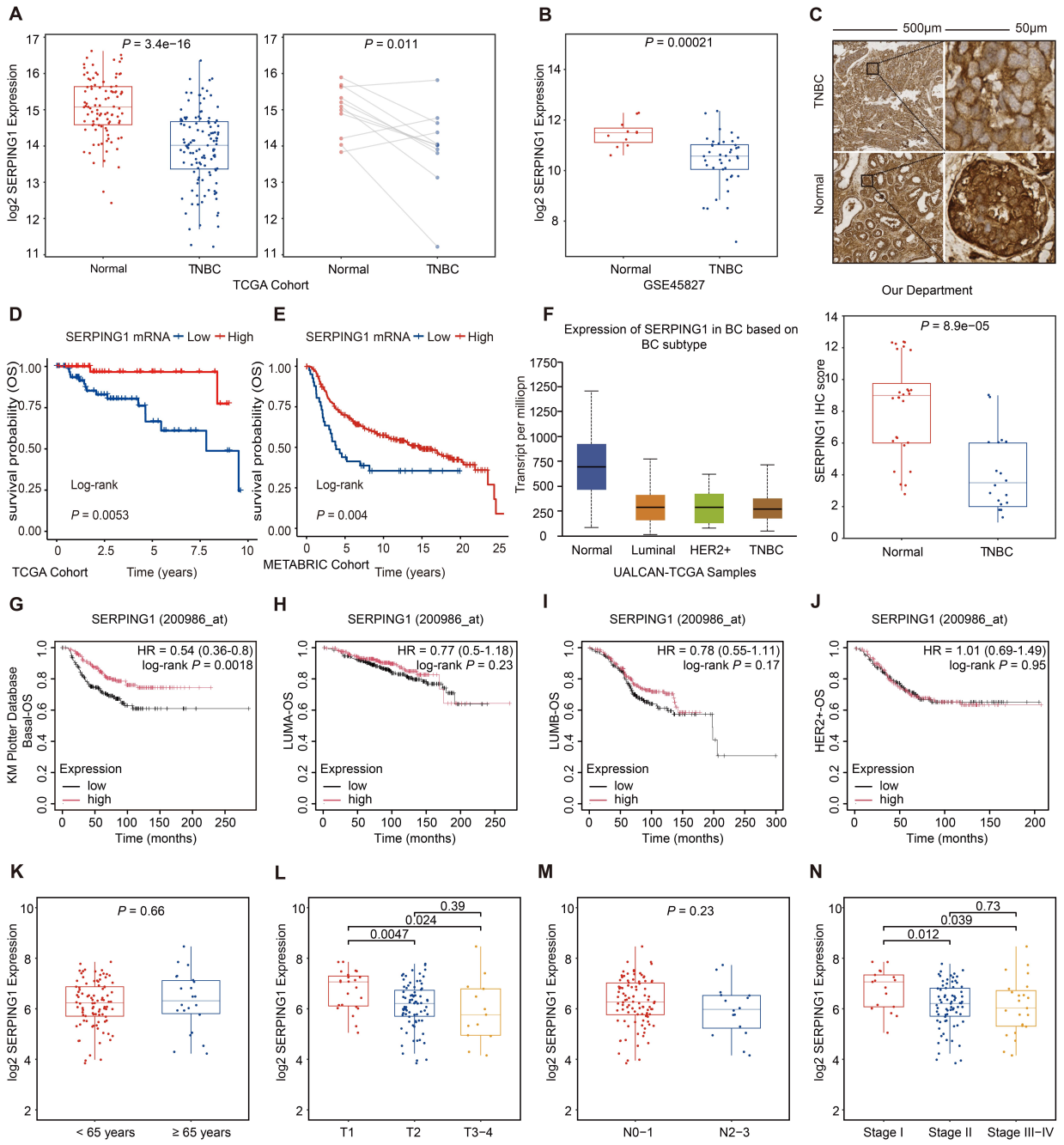

Fig. 2. Downregulated *SERPING1* in TNBC leads to advanced tumor stage and poor prognosis. (A) Box plots of *SERPING1* expression in normal tissues and TNBC (left); Dot plots of paired normal and TNBC (right) based on TCGA database. (B) Box plots of *SERPING1* expression in normal tissues and TNBC according to GSE45827. (C) Representative images of SERPING1 stained by IHC in TNBC (top) and normal mammary (bottom) were shown on the top, and Box plots of the distribution of IHC score were shown on the bottom. Scale bar = 500 μm (Left); Scale bar = 50 μm (Right). (D–F) Kaplan-Meier survival curve of OS based on (D) TCGA and (E) METABRIC database. (F) Box plots of *SERPING1* expression in normal tissues and BC subtype using the UALCAN tool. (G–J) Kaplan-Meier survival curve of OS based on Kaplan-Meier plotter database for (G) Basal BC, (H) LUMA BC, (I) LUMB BC and (J) HER2+ BC. (K–N) Box plots demonstrating the relationship of *SERPING1* expression with (K) patient age, (L) tumor size, (M) lymph node involvement, and (N) cancer staging. Paired *t* test was used for paired normal-TNBC analysis. Other data were analyzed for statistical significance using Wilcox test. Two-sided *p*-values < 0.05 were considered to be statistically significant. TNBC, triple-negative breast cancer; BC, breast cancer; IHC, immunohistochemistry; OS, overall survival; LUMA, luminal-A; LUMB, luminal-B; HER2+, human epidermal growth factor receptor 2-positive.

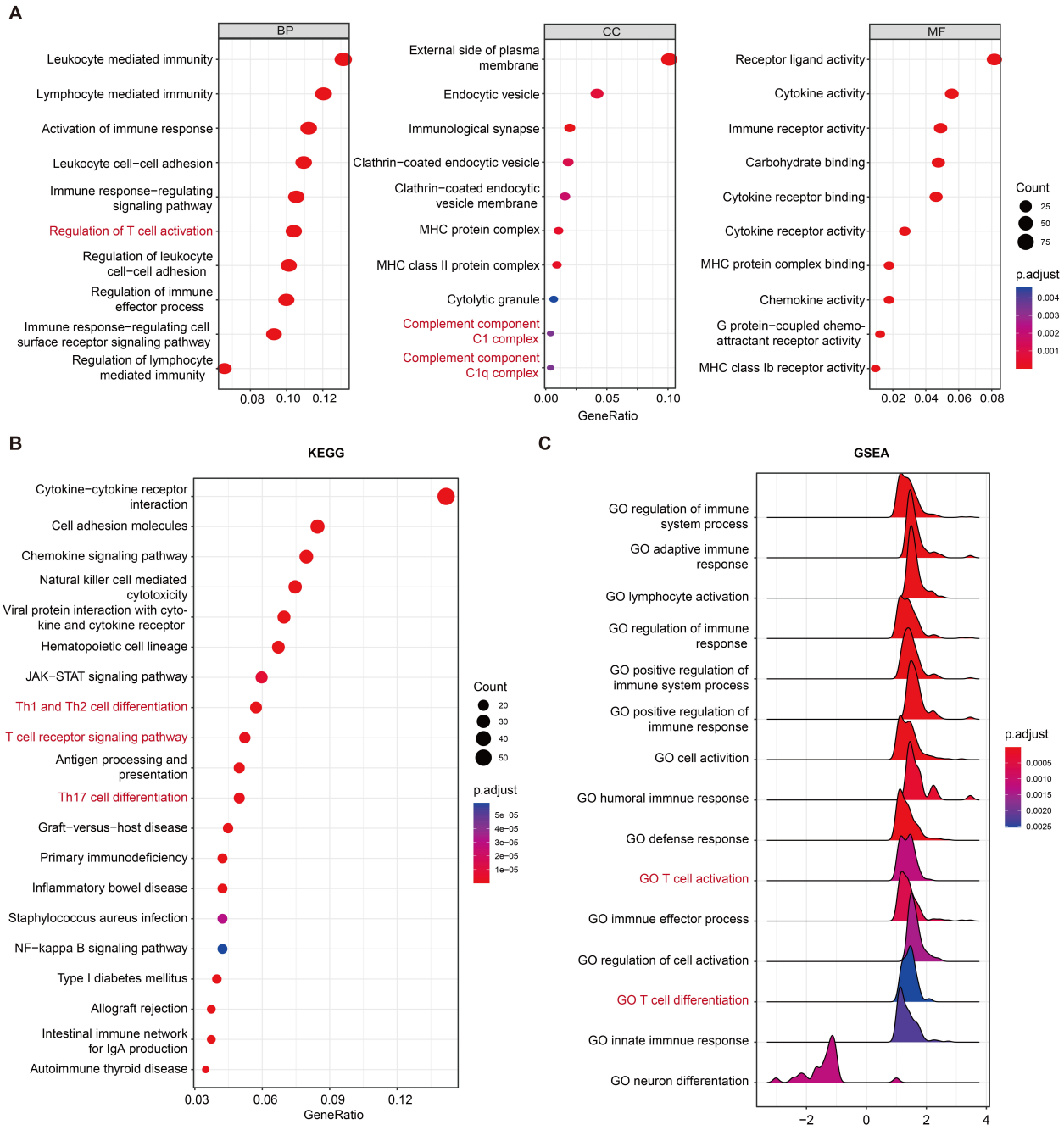

Fig. 3. *SERPING1* is involved in regulating multiple immune-related signaling pathways. (A) GO, (B) KEGG and (C) GSEA enrichment of SERPING1-related genes. GO, gene ontology; BP, biological processes; CC, cellular component; MF, molecular function; KEGG, kyoto encyclopedia of genes and genomes; GSEA, gene set enrichment analysis.

hibited a significantly higher IPS score and a lower exclusion score, indicating a stronger likelihood of response to immunotherapy (Fig. 5B,C). To further validate the immune association of *SERPING1*, we analyzed data from a melanoma immunotherapy cohort (GSE91061), which revealed significantly higher *SERPING1* expression in responders compared with non-responders (Fig. 5D). Consistently, analysis of the IMvigor210 cohort, a widely used benchmark dataset for immunotherapy studies, showed that high *SERPING1* expression was associated with favorable prognosis and improved immunotherapy response (Fig. 5E,F).

Subsequently, we compared the predictive performance of *SERPING1* with established biomarkers, including *CD274* and TILs. In both the GSE91061 and IMvigor210 cohorts, *SERPING1* achieved AUC values comparable to those of *CD274* and TILs. Furthermore, incorporating *SERPING1* into combined models with *CD274* and/or TILs modestly improved predictive performance (Fig. 5G,H).

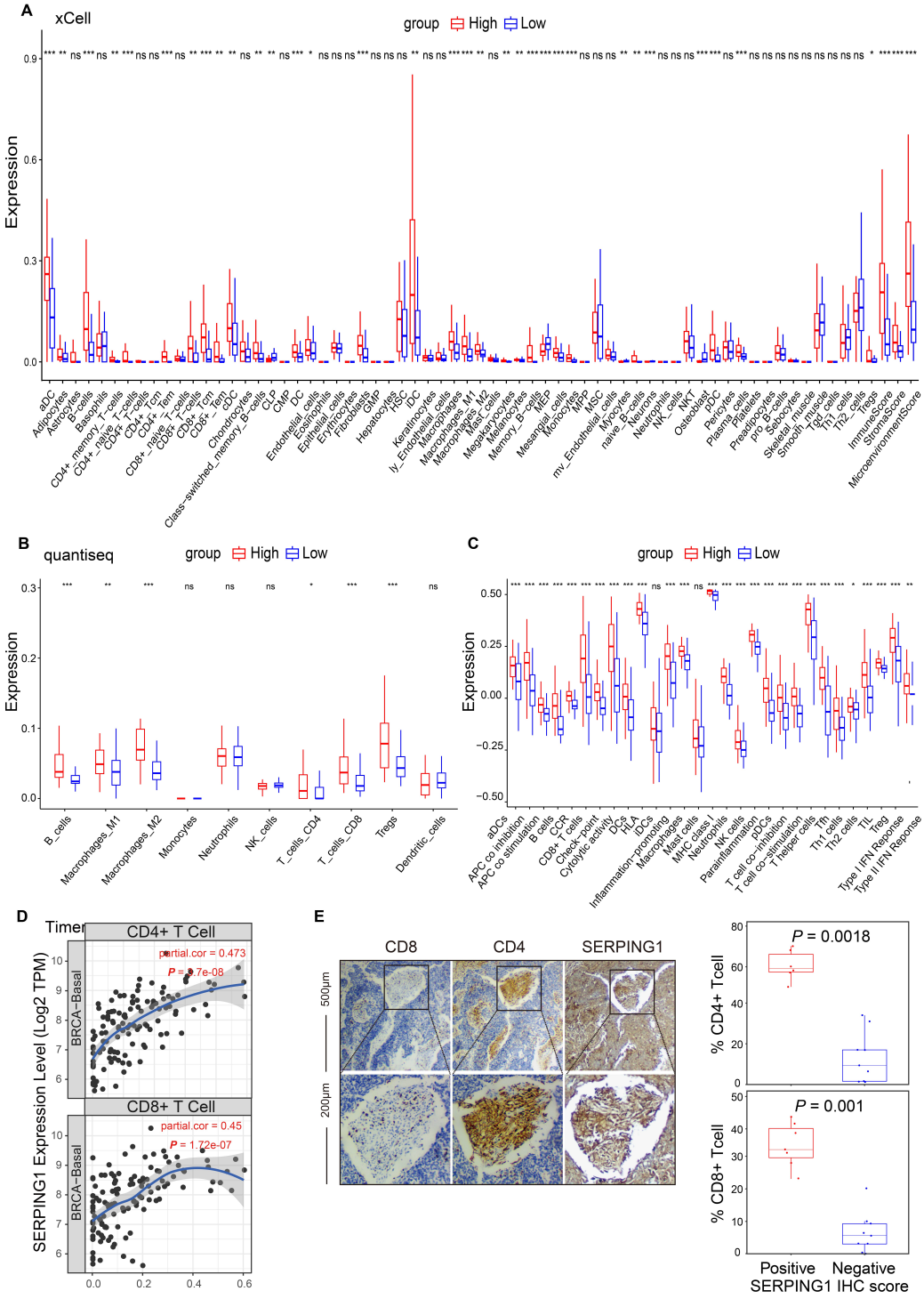

Fig. 4. *SERPING1* is markedly associated with the infiltration of anticancer immune cells in tumors. (A–C) Comparison of immune infiltration between high and low *SERPING1* expression groups was performed via (A) xCell and (B) quantiseq mode. (C) ssGSEA analysis based on 29 immune signatures. (D) Correlation between *SERPING1* expression and infiltration of CD4+ (top) and CD8+ (bottom) T cells in basal BRCA. (E) Representative IHC staining of CD8 (left), CD4 (middle), and SERPING1 (right) in TNBC samples was shown on the left, and Box plots display the percentage of CD4+ (top) or CD8+ (bottom) T cells in TNBC tumor tissue sections were shown on the right. The difference between groups was analyzed using the Wilcox test. Scale bar = 50 μm (Up); Scale bar = 200 μm (Down). Two-sided *p*-values < 0.05 were considered to be statistically significant. **p*-value < 0.05, ***p*-value < 0.01, ****p*-value < 0.001, ns = not significant. ssGSEA, single sample gene set enrichment analysis; BRCA, breast cancer; IHC, immunohistochemistry; TNBC, triple-negative breast cancer.

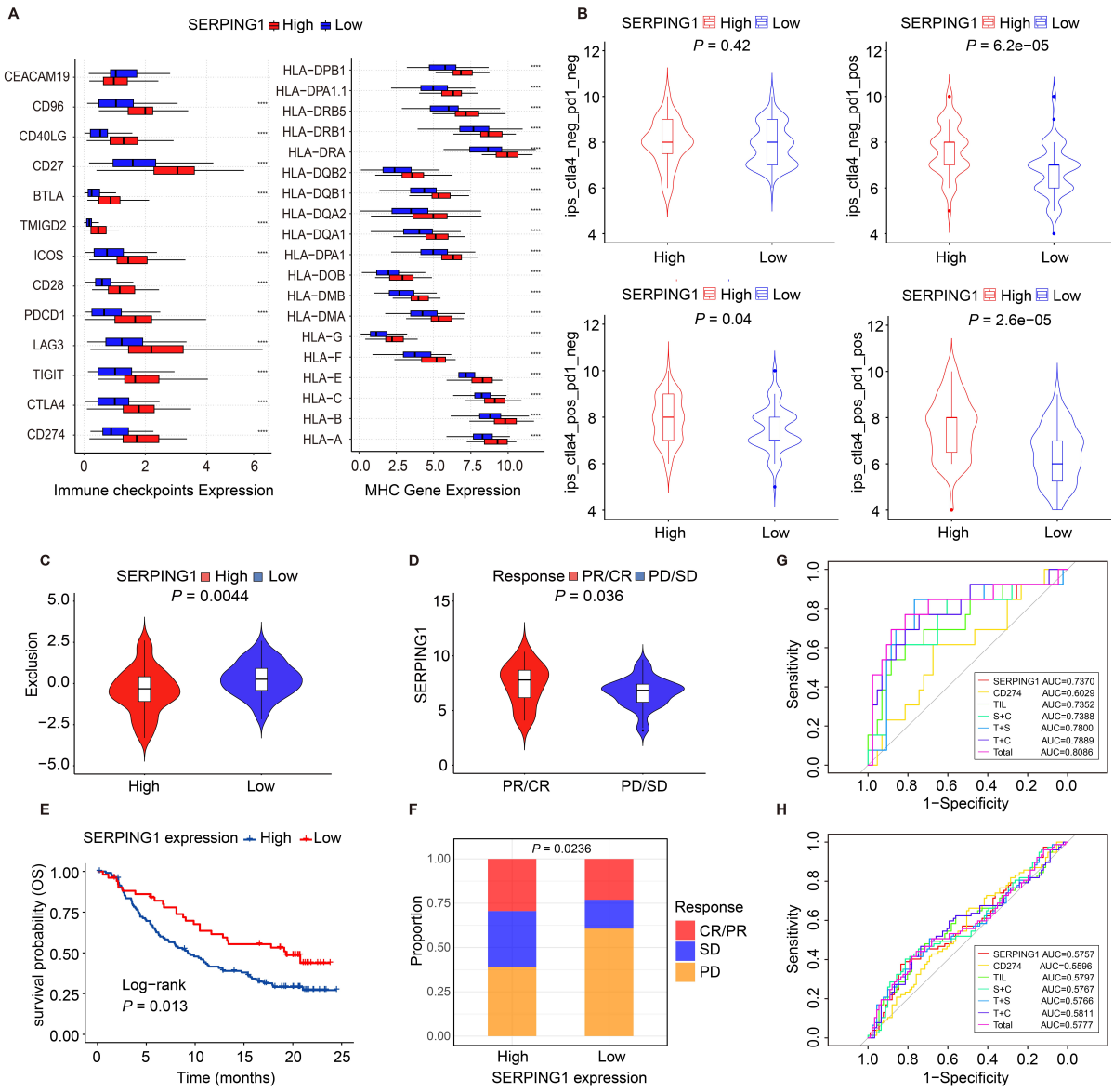

Fig. 5. High *SERPING1* expression is sensitive to tumor immunotherapy. (A) Box plots demonstrating the abundance of immune checkpoints and MHC molecules between high and low *SERPING1* expression groups. (B,C) Violin plots of (B) IPS scores and (C) exclusion scores between high and low *SERPING1* expression groups. (D) Violin plots of *SERPING1* expression across different immunotherapy response groups in GSE91061 dataset. (E) Kaplan-Meier survival curve of OS based on IMvigor210 cohort. (F) Stacked bar plots of immunotherapy reactivity between high and low *SERPING1* expression groups in IMvigor210 cohort. (G,H) ROC curves of the predictive performance of *SERPING1*, *CD274*, TILs, SERPING1+*CD274* (S+C), TILs+*SERPING1* (T+S), TILs+*CD274* (T+C) and TILs+*SERPING1*+*CD274* (Total) based on (G) GSE91061 and (H) IMvigor210 cohort. The difference between groups was analyzed using the Wilcox test. Two-sided *p*-values < 0.05 were considered to be statistically significant. ****p-value < 0.0001. MHC, major histocompatibility complex; IPS, immunophenoscore; PR/CR, partial response/complete response; PD/SD, progression disease/stable disease.

3.6 Single-cell RNA Sequencing Profiles Clarified the Contribution of SERPING1 to Immune Infiltration

To examine the regulatory role of *SERPING1* on tumor immunity at single-cell resolution, we performed dimensionality reduction analysis on scRNA-seq data containing 9 TNBC samples from GSE176078. 15 cell clusters were annotated and assigned to 9 cell types, namely B cells, CD4+ T cells, CD8+ T cells, DC, endothelial cells, epithelial cells, CAFs, macrophages and natural killer (NK) cells (Fig. 6A and **Supplementary Fig. 4A**). *SERPING1* was mainly expressed in CAFs, and it was less expressed in macrophages, endothelial cells and DC, which was consistent with the result of higher immune scores and higher proportions of these cells in high *SERPING1* group (Fig. 6B).

CAFs were then isolated and re-clustered into 8 subpopulations (**Supplementary Fig. 4B**). Based on canonical marker genes, these subpopulations were annotated as antigen-presenting CAFs (apCAFs), inflammatory CAFs (iCAFs), myofibroblastic CAFs (myCAFs), vascular CAFs (vCAFs) and a distinct SERPING1-KRT8+ CAF population (Fig. 6C,D). This SERPING1-KRT8+ subset could not be assigned to any established CAF subtypes. Notably, *SERPING1* was expressed in all other CAF subtypes but was absent in the SERPING1-KRT8+ subset (Fig. 6E). Cell communication analysis revealed that SERPING1+ apCAFs exhibited the most interactions with immune cells (Fig. 6F). Ligand-receptor interaction analysis indicated that these apCAFs engaged extensively with T cells via the MHC-I, MHC-II, and CXCL signaling pathways, all of which have been previously implicated in immune activation. In contrast, the MIF signaling pathway, associated with immunosuppression, was significantly enriched in the crosstalk of SERPING1-KRT8+ CAFs (Fig. 6G,H). Furthermore, SERPING-KRT8+ CAFs displayed reduced MHC-I expression and significantly fewer interactions with CD8+ T cells compared to all SERPING1+ CAF subtypes (Fig. 6G,H and **Supplementary Fig. 4C**). These findings indicated that *SERPING1* loss in CAFs may impair immune activation with TNBC TME.

4. Discussion

TNBC is the most aggressive subtype of BC, with limited treatment strategies and high immunogenicity. Recently, anti-PD-L1 antibodies have been approved for the treatment of both early- and late-TNBC, demonstrating significant benefits. Although the application of molecular targeted therapies and ICIs has extended survival in some patients with advanced TNBC, treatment resistance and relapse remain frequent due to the complexity of the TME. Within the TME, immune cells, remodeled ECM, soluble factors, epigenetic alterations, and reprogrammed fibroblasts interact to shape the anti-tumor immune response, driving tumor initiation, progression, and metastasis. Therefore, an in-depth investigation of the role of TME in TNBC is crucial for optimizing therapeutic strategies and enhancing immunotherapy efficacy.

In our study, by integrating clinical data, bioinformatics analyses and IHC validation, we identify *SERPING1* as a potential biomarker associated with immune infiltration in TNBC. *SERPING1* encodes a serine protease inhibitor that inactivates C1r and C1s proteases of the C1 complex in the classical complement pathway, thereby suppressing complement activation. Initially, *SERPING1* was primarily studied in the context of hereditary angioedema and partial complement component deficiency. Recently, its role in various tumors has gained increasing attention [20,33]. In BC, low *SERPING1* expression was reported as an early diagnostic marker for bone metastasis and was significantly downregulated in metastatic lymph nodes of hormone receptor-positive BC [34,35]. However, the specific function and mechanism of *SERPING1* in TNBC remain unclear. Our study revealed that SERPING1 expression was decreased in TNBC, with low expression strongly associated with advanced stage and poor patient survival. These findings are consistent with studies in prostate and gastric cancers, indicating that *SERPING1* loss may act as an adverse factor in the progression of multiple tumor types [21,36,37].

Research by Shen *et al.* [38] demonstrated that SERPING1 could inhibit lung cancer progression via the TSC2/mTOR signaling pathway and *SERPING1* was linked to immunotherapy response. In this study, GO and KEGG functional enrichment analyses indicated that SERPING1-related genes were primarily involved in immune regulatory pathways, suggesting a potential role of *SERPING1* in anti-tumor immune regulation in TNBC. In addition, we applied multiple robust bioinformatics approaches to analyze the immune microenvironment of TNBC samples from the TCGA cohort. Our results revealed that high *SERPING1* expression was significantly associated with an immune-activated TME, characterized by elevated infiltration of anti-tumor immune cells, including CD8+ T cells, CD4+ T cells, M1 macrophages, and DC. Immunotherapy response analysis showed that the high *SERPING1* group exhibited significantly increased levels of MHC molecules, immune checkpoint genes, and IPS, indicating enhanced immune responsiveness. Moreover, immunotherapy efficacy analysis in two independent external cohorts further supported its potential as a biomarker for immunotherapy prediction.

GSEA analysis further indicated that SERPING1-related genes are primarily enriched in T cell regulatory pathways, thereby enhancing anti-tumor immunity through activation of T cells within the TME. To validate this hypothesis, IHC staining was performed on tissue microarrays from our hospital. The results demonstrated that infiltration levels of CD4+ and CD8+ T cells were significantly higher in the SERPING1-positive group compared with the SERPING1-negative group. Subsequently, scRNA-seq analysis revealed that *SERPING1* was predominantly expressed in CAFs. CAFs are the most abundant cellular component of the TME and constitute a highly heterogeneous population derived from multiple cell types. They exert complex functions in tumor progression by secreting soluble factors, releasing exosomes, providing nutrients, remodeling the ECM, and modulating immune cell activity [15]. Recent studies have clarified the functions of distinct CAF subpopulations in BC, which can be roughly classified into myCAFs, iCAFs and apCAFs [39]. MyCAFs are mainly located near tumor cells, highly express ECM-related proteins, and promote the formation of an immunosuppressive TME. In contrast, iCAFs are situated farther from tumor cells, exhibit low α-SMA expression, and secrete inflammatory factors such as IL-6, IL-8, IL-11, and LIF, which can facilitate cytotoxic T cell recruit-

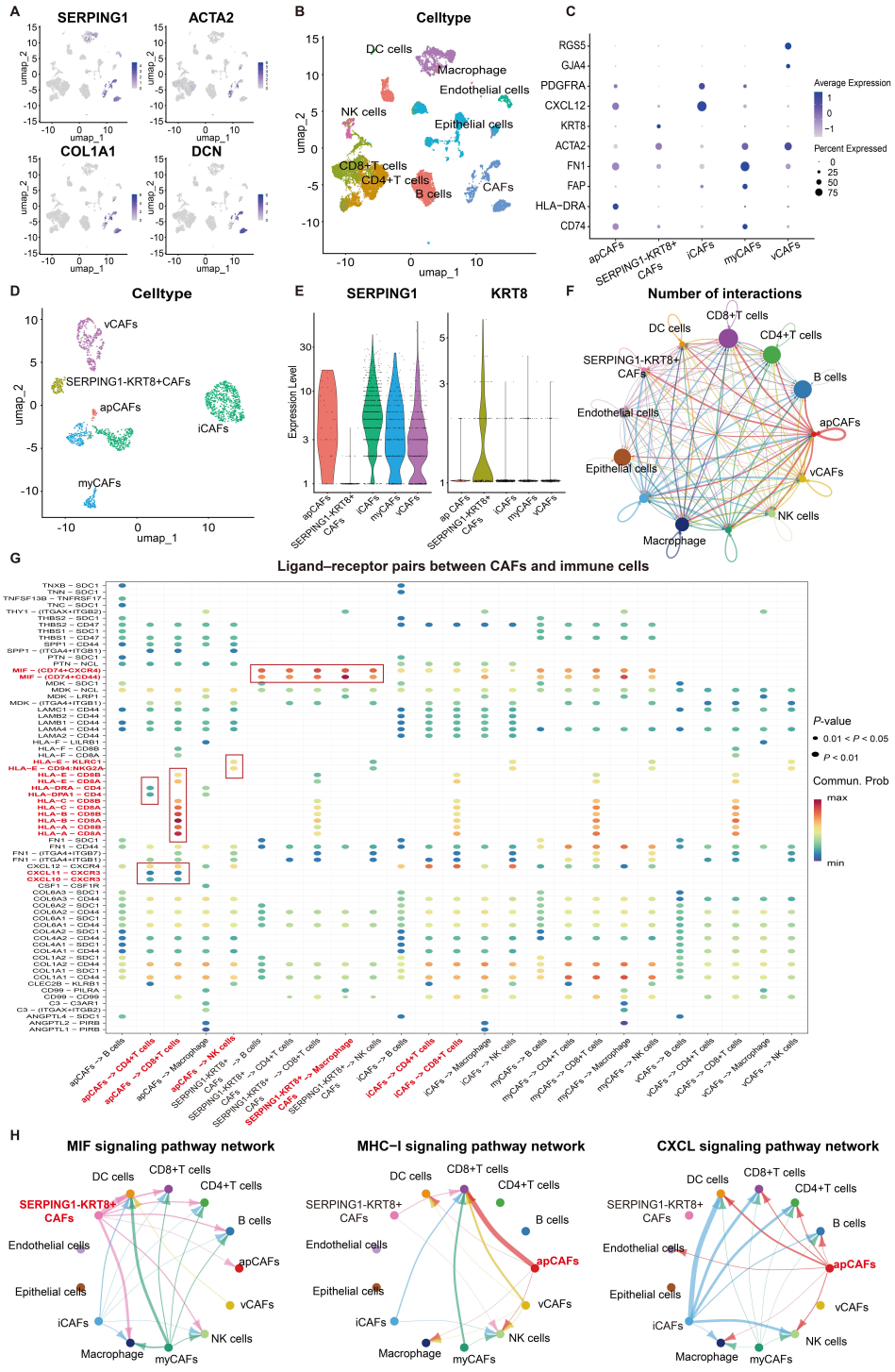

Fig. 6. The contribution of *SERPING1* to cellular communication at the single-cell level. (A) The UMAP plots exhibit the expression levels of *SERPING1* and CAFs marker genes. (B) UMAP plot for the dimension reduction and visualization of 9 cell types within the TME. (C) Expression levels of marker genes for each CAFs subtype. (D) UMAP plot for the dimension reduction and visualization of 5 CAFs subtypes. (E) Violin plots of *SERPING1* and *KRT8* in each CAFs subtype. (F) The cellular interaction network between different cell types in TNBC. (G) Bubble plots exhibiting significant interactions between 5 CAFs subtypes with other immune cells by the ligand-receptor pairs. (H) The cellular interaction network between different cell types in various signaling pathways, including MIF (left), MHC-I (middle) and CXCL (right) signaling pathways. UMAP, uniform manifold approximation and projection; TNBC, triple-negative breast cancer; TME, tumor microenvironment; MIF, macrophage migration inhibitory factor; MHC-I, major histocompatibility complex-I; CXCL, chemokine ligand; CAFs, cancer-associated fibroblasts; apCAFs, antigen-presenting CAFs; iCAFs, inflammatory CAFs; myCAFs, myofibroblastic CAFs; vCAFs, vascular CAFs.

ment [40,41]. CAFs have also been implicated in modulating responses to immunotherapy in TNBC. Tian *et al*. [42] reported that apCAFs expressing MHC II molecules and CD74A are significantly correlated with enhanced immune infiltration in TNBC. Moreover, reprogramming CAFs has been shown to improve the efficacy of immunotherapy in TNBC [43,44]. These findings indicate that different CAF subpopulations may play opposing roles in BC progression and immunomodulation, highlighting the potential of targeting specific CAF subsets as a therapeutic strategy.

Cell communication analysis indicated that SERPING1+ apCAFs exhibit strong interactions with anti-tumor immune cells, including CD8+ T cells, CD4+ T cells, and NK cells. Consistent with our findings, previous studies have demonstrated that SERPING1+ CAFs are closely associated with T cell infiltration in nasopharyngeal carcinoma and melanoma [45–47]. In contrast, ligand-receptor interaction analysis of SERPING1-KRT8+ CAFs revealed enrichment of the MIF signaling pathway, which has been reported to promote immunosuppression by inhibiting p53 expression and activating multiple oncogenic signaling pathways [48,49]. Compared with all SERPING1+ CAF subtypes, SERPING1-KRT8+ CAFs exhibited markedly fewer interactions with T cells and lacked enrichment of CXCL signaling pathways. Moreover, previous research reported that KRT8 upregulation in CAFs was associated with enhanced tumor growth and metastasis [50]. Differential expression between SERPING1+ apCAFs and SERPING1-KRT8+ CAFs revealed enrichment in cytokine secretion pathways (**Supplementary Fig. 5**). Collectively, our findings indicated that the reduced SERPING1 expression in CAFs may diminish cytokine and chemokine production, limit immune cell infiltration, and consequently promote an immunosuppressive microenvironment associated with poor prognosis in TNBC. However, the precise molecular mechanisms of *SERPING1* in TNBC warrant further investigation.

To the best of our knowledge, this is the first study to systematically elucidate the role of *SERPING1* in TNBC patients. However, there are still some limitations. First, the IHC validation cohort included only 18 TNBC samples due to limited tissue availability and strict inclusion criteria. Second, although our conclusions were supported by multiple public datasets and single-cell analyses, functional experiments are needed to verify the role of *SERPING1* in CAFs. Additionally, the molecular mechanisms underlying SERPING1-mediated immune regulation in TNBC remained to be fully elucidated. Further studies with larger clinical cohorts and mechanistic experiments are warranted to validate and extend these findings.

5. Conclusion

In conclusion, our analysis indicated that *SERPING1* is a favorable prognostic factor, with its expression positively correlated with immune activity and response to immunotherapy in TNBC. Mechanically, SERPING1+ apCAFs could promote immune activation through interactions with T cells in the TME. These findings highlighted *SERPING1* as a potential biomarker for immune infiltration and prognostic prediction in TNBC. We expected to provide the foundation for further in-depth research on *SERPING1* in TNBC.

Disclosure

The paper is listed as, “Integrated single-cell and bulk RNA sequencing identifies SERPING1 as an immune infiltration regulator and therapeutic target in Triple-negative breast cancer ” as a preprint on (SSRN) at: (https://www.researchsquare.com/article/rs-7064973/v1.pdf).

Availability of Data and Materials

The datasets generated and/or analyzed during the current study are available in the TCGA database on the Xena website (http://xena.ucsc.edu/), the GEO (https://www.ncbi.nlm.nih.gov/geo/), the METABRIC database (https://www.bccrc.ca/dept/mo/), the Kaplan-Meier plotter (KM plotter, https://kmplot.com/analysis/), and the UALCAN tool (https://ualcan.path.uab.edu/). The datasets used and analyzed during the current study are available from the corresponding author on reasonable request. Further inquiries can be directed to the corresponding authors.

Author Contributions

YHS and BLG were responsible for conception and design of this study, YHS wrote the main manuscript text, YHJ, JWL, RZG, ABH, YQD and YSL collected and analyzed datasets, XLW, MCL, HYZ, ZYR and YLL prepared all figures. WLC, ZBF, YYJ, YLC and DLC interpreted the data, YYJ prepared **Supplementary Materials**. All authors reviewed the manuscript. All authors contributed to editorial changes in the manuscript. All authors read and approved the final manuscript. All authors have participated sufficiently in the work and agreed to be accountable for all aspects of the work.

Ethics Approval and Consent to Participate

This study was approved by the Ethics Committee of HMU (Ethics Code: YJSDW2024-260) on May 29, 2024. All participants provided written informed consent prior to enrolment in the study. This research was conducted ethically in accordance with the World Medical Association Declaration of Helsinki.

Acknowledgment

The authors thank the Department of Pathology at the Second Affiliated Hospital of Harbin Medical University for their professional assistance. We acknowledged the TCGA database, GEO database, Kaplan-Meier Plotter database and UALCAN tool for providing their platforms and contributors for uploading their meaningful datasets.

Funding

This study was funded by grants from the National Natural Science Foundation of China (81872135).

Conflict of Interest

The authors declare no conflict of interest.

Supplementary Material

Supplementary material associated with this article can be found, in the online version, at https://doi.org/10.31083/FBL47089.

References

[1] Dent R, Trudeau M, Pritchard KI, Hanna WM, Kahn HK, Sawka CA, *et al*. Triple-negative breast cancer: clinical features and patterns of recurrence. Clinical Cancer Research: an Official Journal of the American Association for Cancer Research. 2007; 13: 4429–4434. https://doi.org/10.1158/1078-0432.CCR-06-3045.

[2] Cancer Genome Atlas Network. Comprehensive molecular portraits of human breast tumours. Nature. 2012; 490: 61–70. https://doi.org/10.1038/nature11412.

[3] Lehmann BD, Bauer JA, Chen X, Sanders ME, Chakravarthy AB, Shyr Y, *et al*. Identification of human triple-negative breast cancer subtypes and preclinical models for selection of targeted therapies. The Journal of Clinical Investigation. 2011; 121: 2750–2767. https://doi.org/10.1172/JCI45014.

[4] Morad G, Helmink BA, Sharma P, Wargo JA. Hallmarks of response, resistance, and toxicity to immune checkpoint blockade. Cell. 2021; 184: 5309–5337. https://doi.org/10.1016/j.cell.2021.09.020.

[5] Bareche Y, Kelly D, Abbas-Aghababazadeh F, Nakano M, Esfahani PN, Tkachuk D, *et al*. Leveraging big data of immune checkpoint blockade response identifies novel potential targets. Annals of Oncology: Official Journal of the European Society for Medical Oncology. 2022; 33: 1304–1317. https://doi.org/10.1016/j.annonc.2022.08.084.

[6] Vikas P, Borcherding N, Zhang W. The clinical promise of immunotherapy in triple-negative breast cancer. Cancer Management and Research. 2018; 10: 6823–6833. https://doi.org/10.2147/CMAR.S185176.

[7] Schmid P, Rugo HS, Adams S, Schneeweiss A, Barrios CH, Iwata H, *et al*. Atezolizumab plus nab-paclitaxel as first-line treatment for unresectable, locally advanced or metastatic triple-negative breast cancer (IMpassion130): updated efficacy results from a randomised, double-blind, placebo-controlled, phase 3 trial. The Lancet. Oncology. 2020; 21: 44–59. https://doi.org/10.1016/S1470-2045(19)30689-8.

[8] Cortes J, Cescon DW, Rugo HS, Nowecki Z, Im SA, Yusof MM, *et al*. Pembrolizumab plus chemotherapy versus placebo plus chemotherapy for previously untreated locally recurrent inoperable or metastatic triple-negative breast cancer (KEYNOTE-355): a randomised, placebo-controlled, double-blind, phase 3 clinical trial. Lancet (London, England). 2020; 396: 1817–1828. https://doi.org/10.1016/S0140-6736(20)32531-9.

[9] Schmid P, Adams S, Rugo HS, Schneeweiss A, Barrios CH, Iwata H, *et al*. Atezolizumab and Nab-Paclitaxel in Advanced Triple-Negative Breast Cancer. The New England Journal of Medicine. 2018; 379: 2108–2121. https://doi.org/10.1056/NEJMoa1809615.

[10] Jin MZ, Jin WL. The updated landscape of tumor microenvironment and drug repurposing. Signal Transduction and Targeted Therapy. 2020; 5: 166. https://doi.org/10.1038/s41392-020-00280-x.

[11] Stanton SE, Disis ML. Clinical significance of tumor-infiltrating lymphocytes in breast cancer. Journal for Immunotherapy of Cancer. 2016; 4: 59. https://doi.org/10.1186/s40425-016-0165-6.

[12] Dhas N, Kudarha R, Kulkarni S, Soman S, Navti PD, Kulkarni J, *et al*. Nanoengineered Platform-Based Microenvironment-Triggered Immunotherapy in Cancer Treatment. Front Biosci (Landmark Ed). Frontiers in Bioscience-Landmark. 2024; 29: 349. https://doi.org/10.31083/j.fbl2910349.

[13] Binnewies M, Roberts EW, Kersten K, Chan V, Fearon DF, Merad M, *et al*. Understanding the tumor immune microenvironment (TIME) for effective therapy. Nature Medicine. 2018; 24: 541–550. https://doi.org/10.1038/s41591-018-0014-x.

[14] Kalluri R. The biology and function of fibroblasts in cancer. Nature Reviews. Cancer. 2016; 16: 582–598. https://doi.org/10.1038/nrc.2016.73.

[15] Toullec A, Gerald D, Despouy G, Bourachot B, Cardon M, Lefort S, *et al*. Oxidative stress promotes myofibroblast differentiation and tumour spreading. EMBO Molecular Medicine. 2010; 2: 211–230. https://doi.org/10.1002/emmm.201000073.

[16] Mao X, Xu J, Wang W, Liang C, Hua J, Liu J, *et al*. Crosstalk between cancer-associated fibroblasts and immune cells in the tumor microenvironment: new findings and future perspectives. Molecular Cancer. 2021; 20: 131. https://doi.org/10.1186/s12943-021-01428-1.

[17] Ma X, Shan H, Chen Z, Shao R, Han N. Programmed cell death-related prognostic genes mediate dysregulation of the immune microenvironment in triple-negative breast cancer. Frontiers in Immunology. 2025; 16: 1563630. https://doi.org/10.3389/fimmu.2025.1563630.

[18] Davis AE, 3rd, Cai S, Liu D. C1 inhibitor: biologic activities that are independent of protease inhibition. Immunobiology. 2007; 212: 313–323. https://doi.org/10.1016/j.imbio.2006.10.003.

[19] Starcević D, Jelić-Ivanović Z, Kalimanovska V. Plasma C1 inhibitor in malignant diseases: functional activity versus concentration. Annals of Clinical Biochemistry. 1991; 28 (Pt 6): 595–598. https://doi.org/10.1177/000456329102800609.

[20] Su H, Chen Y, Wang W. Novel prognostic model of complement and coagulation cascade-related genes correlates with immune environment and drug sensitivity in hepatocellular carcinoma. Heliyon. 2024; 10: e38230. https://doi.org/10.1016/j.heliyon.2024.e38230.

[21] Peng S, Du T, Wu W, Chen X, Lai Y, Zhu D, *et al*. Decreased expression of serine protease inhibitor family G1 (SERPING1) in prostate cancer can help distinguish high-risk prostate cancer and predicts malignant progression. Urologic Oncology. 2018; 36: 366.e1–366.e9. https://doi.org/10.1016/j.urolonc.2018.05.021.

[22] Janssen CW, Jr, Lie RT, Maartmann-Moe H, Matre R. Serum C1-esterase inhibitor, an essential and independent prognosticator of gastric carcinoma. British Journal of Cancer. 1989; 60: 589–591. https://doi.org/10.1038/bjc.1989.319.

[23] Chandrashekar DS, Karthikeyan SK, Korla PK, Patel H, Shovon AR, Athar M, *et al*. UALCAN: An update to the integrated cancer data analysis platform. Neoplasia (New York, N.Y.). 2022; 25: 18–27. https://doi.org/10.1016/j.neo.2022.01.001.

[24] Yi J, Zhong W, Wu H, Feng J, Zouxu X, Huang X, *et al*. Identification of Key Genes Affecting the Tumor Microenvironment and Prognosis of Triple-Negative Breast Cancer. Frontiers in Oncology. 2021; 11: 746058. https://doi.org/10.3389/fonc.2021.746058.

[25] He Y, Jiang Z, Chen C, Wang X. Classification of triple-negative breast cancers based on Immunogenomic profiling. Journal of Experimental & Clinical Cancer Research: CR. 2018; 37: 327. https://doi.org/10.1186/s13046-018-1002-1.

[26] Liu XS, Zhou LM, Yuan LL, Gao Y, Kui XY, Liu XY, *et al*. NPM1 Is a Prognostic Biomarker Involved in Immune Infiltration of Lung Adenocarcinoma and Associated With m6A Modification and Glycolysis. Frontiers in Immunology. 2021; 12: 724741. https://doi.org/10.3389/fimmu.2021.724741.

[27] Li Y, Feng J, Wang T, Li M, Zhang H, Rong Z, *et al*. Construction of an immunogenic cell death-based risk score prognosis model in breast cancer. Frontiers in Genetics. 2022; 13: 1069921. https://doi.org/10.3389/fgene.2022.1069921.

[28] Jiang P, Gu S, Pan D, Fu J, Sahu A, Hu X, *et al*. Signatures of T cell dysfunction and exclusion predict cancer immunotherapy response. Nature Medicine. 2018; 24: 1550–1558. https://doi.org/10.1038/s41591-018-0136-1.

[29] Charoentong P, Finotello F, Angelova M, Mayer C, Efremova M, Rieder D, *et al*. Pan-cancer Immunogenomic Analyses Reveal Genotype-Immunophenotype Relationships and Predictors of Response to Checkpoint Blockade. Cell Reports. 2017; 18: 248–262. https://doi.org/10.1016/j.celrep.2016.12.019.

[30] Langfelder P, Horvath S. WGCNA: an R package for weighted correlation network analysis. BMC Bioinformatics. 2008; 9: 559. https://doi.org/10.1186/1471-2105-9-559.

[31] Hu A, Liu Y, Zhang H, Wang T, Zhang J, Cheng W, *et al*. BPIFB1 promotes metastasis of hormone receptor-positive breast cancer via inducing macrophage M2-like polarization. Cancer Science. 2023; 114: 4157–4171. https://doi.org/10.1111/cas.15957.

[32] Wang X, Su W, Tang D, Jing J, Xiong J, Deng Y, *et al*. An Immune-Related Gene Prognostic Index for Triple-Negative Breast Cancer Integrates Multiple Aspects of Tumor-Immune Microenvironment. Cancers. 2021; 13: 5342. https://doi.org/10.3390/cancers13215342.

[33] Hsieh CC, Wu YH, Chen YL, Wang CI, Li CJ, Liu IH, *et al*. SERPING1 Reduces Cell Migration via ERK-MMP2-MMP-9 Cascade in Sorafenib- Resistant Hepatocellular Carcinoma. Environmental Toxicology. 2025; 40: 318–327. https://doi.org/10.1002/tox.24434.

[34] Popeda M, Markiewicz A, Stokowy T, Szade J, Niemira M, Kretowski A, *et al*. Reduced expression of innate immunity-related genes in lymph node metastases of luminal breast cancer patients. Scientific Reports. 2021; 11: 5097. https://doi.org/10.1038/s41598-021-84568-0.

[35] Zhao Z, Yang H, Ji G, Su S, Fan Y, Wang M, *et al*. Identification of hub genes for early detection of bone metastasis in breast cancer. Frontiers in Endocrinology. 2022; 13: 1018639. https://doi.org/10.3389/fendo.2022.1018639.

[36] O-charoenrat P, Rusch V, Talbot SG, Sarkaria I, Viale A, Socci N, *et al*. Casein kinase II alpha subunit and C1-inhibitor are independent predictors of outcome in patients with squamous cell carcinoma of the lung. Clinical Cancer Research: an Official Journal of the American Association for Cancer Research. 2004; 10: 5792–5803. https://doi.org/10.1158/1078-0432.CCR-03-0317.

[37] Liljedahl E, Konradsson E, Gustafsson E, Jonsson KF, Olofsson JK, Osther K, *et al*. Combined anti-C1-INH and radiotherapy against glioblastoma. BMC Cancer. 2023; 23: 106. https://doi.org/10.1186/s12885-023-10583-1.

[38] Shen Y, Dong X, Li X, Shi Z, Shao T, Jiang J, *et al*. WNT inhibitor SP5-mediated SERPING1 suppresses lung adenocarcinoma progression via TSC2/mTOR pathway. Cell Death & Disease. 2025; 16: 103. https://doi.org/10.1038/s41419-025-07440-3.

[39] Sebastian A, Hum NR, Martin KA, Gilmore SF, Peran I, Byers SW, *et al*. Single-Cell Transcriptomic Analysis of Tumor-Derived Fibroblasts and Normal Tissue-Resident Fibroblasts Reveals Fibroblast Heterogeneity in Breast Cancer. Cancers. 2020; 12: 1307. https://doi.org/10.3390/cancers12051307.

[40] Honda CK, Kurozumi S, Fujii T, Pourquier D, Khellaf L, Boissiere F, *et al*. Cancer-associated fibroblast spatial heterogeneity and *EMILIN1* expression in the tumor microenvironment modulate TGF-β activity and CD8$^+$ T-cell infiltration in breast cancer. Theranostics. 2024; 14: 1873–1885. https://doi.org/10.7150/thno.90627.

[41] Croizer H, Mhaidly R, Kieffer Y, Gentric G, Djerroudi L, Leclere R, *et al*. Deciphering the spatial landscape and plasticity of immunosuppressive fibroblasts in breast cancer. Nature Communications. 2024; 15: 2806. https://doi.org/10.1038/s41467-024-47068-z.

[42] Tian J, Li Y, Wang Z, Zhong Y, Yao Y, Sun C. Antigen-presenting CAFs orchestrate immunosuppressive niches via CXCL13-mediated immune cell infiltration dysregulation and prognostic stratification in triple-negative breast cancer. International Immunopharmacology. 2025; 162: 115193. https://doi.org/10.1016/j.intimp.2025.115193.

[43] Zhang Y, Zhou J, Wang Y, Wu Y, Li Y, Wang B, *et al*. Stimuli-responsive polymer-dasatinib prodrug to reprogram cancer-associated fibroblasts for boosted immunotherapy. Journal of Controlled Release: Official Journal of the Controlled Release Society. 2025; 381: 113606. https://doi.org/10.1016/j.jconrel.2025.113606.

[44] Xian P, Zou L, Zhang J, Pan X, Song Y, Nan Y, *et al*. Precision targeted cancer-associated fibroblast nano-regulator enhanced chemo-immunotherapy for triple-negative breast cancer. Biomaterials. 2026; 326: 123679. https://doi.org/10.1016/j.biomaterials.2025.123679.

[45] Jin S, Li R, Chen MY, Yu C, Tang LQ, Liu YM, *et al*. Single-cell transcriptomic analysis defines the interplay between tumor cells, viral infection, and the microenvironment in nasopharyngeal carcinoma. Cell Research. 2020; 30: 950–965. https://doi.org/10.1038/s41422-020-00402-8.

[46] Tirosh I, Izar B, Prakadan SM, Wadsworth MH, 2nd, Treacy D, Trombetta JJ, *et al*. Dissecting the multicellular ecosystem of metastatic melanoma by single-cell RNA-seq. Science (New York, N.Y.). 2016; 352: 189–196. https://doi.org/10.1126/science.aad0501.

[47] Yang W, Liu S, Mao M, Gong Y, Li X, Lei T, *et al*. T-cell infiltration and its regulatory mechanisms in cancers: insights at single-cell resolution. Journal of Experimental & Clinical Cancer Research: CR. 2024; 43: 38. https://doi.org/10.1186/s13046-024-02960-w.

[48] Wen Y, Zhu Y, Zhang C, Yang X, Gao Y, Li M, *et al*. Chronic inflammation, cancer development and immunotherapy. Frontiers in Pharmacology. 2022; 13: 1040163. https://doi.org/10.3389/fphar.2022.1040163.

[49] Figueiredo CR, Azevedo RA, Mousdell S, Resende-Lara PT, Ireland L, Santos A, *et al*. Blockade of MIF-CD74 Signalling on Macrophages and Dendritic Cells Restores the Antitumour Immune Response Against Metastatic Melanoma. Frontiers in Immunology. 2018; 9: 1132. https://doi.org/10.3389/fimmu.2018.01132.

[50] Li X, Song Q, Guo X, Wang L, Zhang Q, Cao L, *et al*. The Metastasis Potential Promoting Capacity of Cancer-Associated Fibroblasts Was Attenuated by Cisplatin via Modulating KRT8. OncoTargets and Therapy. 2020; 13: 2711–2723. https://doi.org/10.2147/OTT.S246235.